UCRL-ID-128006

X-Ray Laser Measurements of Direct Drive Imprint on Vulcan

D. H. Kalantar, E. Wolfrum, J. Zhang, M. H. Key, L. B. DaSilva, A. Demir, N. S. Kim, C. L. S. Lewis, J. Lin, A. MacPhee, D. Neely, B. A. Remington, J. E. Rothenberg, R. Smith, G. J. Tallents, J. Wark, J. Warwick, S. V. Weber

July 1, 1997

Lawrence Livermore National Laboratory

This is an informal report intended primarily for internal or limited external distribution. The opinions and conclusions stated are those of the author and may or may not be those of the Laboratory.

Work performed under the auspices of the U.S. Department of Energy by the Lawrence Livermore National Laboratory under Contract W-7405-Eng-48.

DISCLAIMER

This document was prepared as an account of work sponsored by an agency of the United States Government. Neither the United States Government nor the University of California nor any of their employees, makes any warranty, express or implied, or assumes any legal liability or responsibility for the accuracy, completeness, or usefulness of any information, apparatus, product, or process disclosed, or represents that its use would not infringe privately owned rights. Reference herein to any specific commercial product, process, or service by trade name, trademark, manufacturer, or otherwise, does not necessarily constitute or imply its endorsement, recommendation, or favoring by the United States Government or the University of California. The views and opinions of authors expressed herein do not necessarily state or reflect those of the United States Government or the University of California, and shall not be used for advertising or product endorsement purposes.

This report has been reproduced
directly from the best available copy.

Available to DOE and DOE contractors from the
Office of Scientific and Technical Information
P.O. Box 62, Oak Ridge, TN 37831
Prices available from (615) 576-8401, FTS 626-8401

Available to the public from the
National Technical Information Service
U.S. Department of Commerce
5285 Port Royal Rd.,
Springfield, VA 22161

X-RAY LASER MEASUREMENTS OF DIRECT DRIVE IMPRINT ON VULCAN

D. H. Kalantar[a], E. Wolfrum[b], J. Zhang[c], M. H. Key[a], L. B. DaSilva[a], A. Demir[d], N. S. Kim[b], C. L. S. Lewis[e], J. Lin[d], A. MacPhee[e], D. Neely[b], B. A. Remington[a], J. E. Rothenberg[a], R. Smith[d], G. J. Tallents[d], J. Wark[c], J. Warwick[e], and S. V. Weber[a]

[a]Lawrence Livermore National Laboratory, Livermore, California 94550
[b]Rutherford Appleton Laboratory, Chilton, Didcot, United Kingdom
[c]Clarendon Laboratory, University of Oxford, Oxford, United Kingdom
[d]Department of Physics, University of Essex, Colchester, United Kingdom
[e]Department of Pure and Applied Physics, Queen's University of Belfast, Belfast, United Kingdom

INTRODUCTION

High gain direct drive inertial confinement fusion requires very uniform irradiation of a hollow spherical shell with a layer of fusionable deuterium and tritium on its inner surface. The intensity of laser irradiation builds up in several nanoseconds from an initial 'foot' at ~10^{13} W/cm^2 to more than 10^{15} W/cm^2 during the main drive pulse. Laser ablation of the capsule surface produces a high pressure, accelerating the shell radially inward, and resulting in Rayleigh-Taylor (R-T) growth of surface perturbations originating from both the initial surface roughness of the capsule and from imprint of spatial non-uniformities in the laser drive intensity early in the laser pulse.

The uniformity of illumination on a direct drive implosion capsule is determined on a large scale by the multi-beam irradiation geometry, and on a small scale by beam smoothing techniques. By using a large number of beams (such as the 60 beams of the Omega laser[1] or 48 beam clusters for the NIF[2]), large scale non-uniformities due to the overlap of the laser focal spots are adequately reduced. Random phase plates (RPPs)[3] are introduced to smooth the individual beam focal spots. The spatial intensity variations of the individual beam speckle patterns may be smoothed by spectral dispersion (SSD)[4] with induced spatial incoherence (ISI)[5] or by using partially coherent light.[6]

We performed experiments to study the imprint under conditions simulating the low intensity foot of the pulse on an ignition target, such as designed for the NIF. We used a 0.53 μm laser wavelength, and considered the imprint in thin Al foils due to both a broadband distribution of modes such as those in smoothed speckle patterns, and a single mode optical intensity variation. We characterized the laser imprint using a Ge x-ray laser and multilayer imaging optics, as described previously.[7] In this paper we summarize and compare the multiple and single mode imprinting results.

X-RAY LASER RADIOGRAPHY

To measure early time imprinting prior to the onset of R-T growth, we use the Ge x-ray laser, which lases at 19.6 nm. Since the mass absorption coefficients of all materials are high for this wavelength, we use Al foils, with an L absorption edge at a photon energy just above the x-ray laser energy. With this configuration, we are able to probe 2 μm foils with a high sensitivity to modulation in optical depth. A 50 nm variation in the foil thickness corresponds to a 10% variation in the transmission of the x-ray laser.

We use the x-ray laser as a source of radiation for face-on radiography, as described in reference 7. We image the modulation in optical depth of the directly driven foil target using molybdenum-silicon multilayer optics.[8] A single spherical reflecting optic is used at near normal incidence in combination with a flat mirror at 45° incidence that serves to spectrally filter the image. The multilayer optics relay an image of the transmission of the x-ray laser backlighter through the directly drive foil onto a 16-bit Peltier cooled back-thinned (CCD) with high magnification and high resolution. We characterized the modulation transfer function using gold grid targets, and determined that the resolution is equivalent to that from a 5 μm full width at half maximum (fwhm) Gaussian point spread function.

OPTICAL IRRADIATION PATTERN

We show sample far field images of the irradiation patterns used in these imprint experiments in Fig. 1 These images were recorded as an equivalent focal plane image during the experimental series using photographic film that was pulse calibrated at the 0.53 μm laser wavelength. These images are displayed as fractional modulation in the exposure to represent the time integrated optical smoothing level. In addition, we show the 2-D Fourier transforms of the speckle patterns, which we will discuss later.

In Figs. 1a-c, we show the multimode speckle patterns used for the experiments. We show a static speckle pattern, together with SSD smoothed and ISI smoothed speckle patterns at 0.53 μm. The Vulcan beam was f/10, which provides a speckle size of about 10 microns. The imprint beam was incident of the Al foil at 16° off-normal, and the pulse shape was 1.0 ns square with a ~100 ps rise. The average intensity within the fwhm spot size was in the range 2-6x10^{12} W/cm^2.

In Fig. 1d, we show a sample optical intensity pattern used for the single mode imprint experiments. This intensity pattern was achieved by interfering the Airy pattern focal spots of two beam segments that were transmitted through 4 x 10 mm rectangular apertures in a beam block inserted into the beam path. The average intensity was 3-10x10^{12} W/cm^2.

The static speckle pattern is an interference pattern from the random phases of the RPP elements. The Fourier transform shown in Fig. 1a is azimuthally symmetric, and it has a theoretical value for the rms modulation of 1.0. We measured an rms modulation of 0.93.

Smoothing by spectral dispersion reduces the modulation of the speckle pattern by spatially dispersing the time varying spectral components of the broadband laser in one dimension. The speckle pattern fluctuates rapidly in one direction, smoothing of the short wavelength structure in that direction, as indicated by the one-dimensional nature of the Fourier transform of the SSD smoothed speckle pattern. We measured a value of 0.25 for the modulation of the SSD smoothed speckle pattern with 0.5 THz bandwidth (measured with a spectrometer at the 0.53 μm laser wavelength).

Spatial incoherence is induced on the 0.5 THz Vulcan beam by inserting a 5x5 array of varying thickness glass plates into the beam path, in addition to the RPP, introducing delays of up to 220 ps on different segments of the beam. The resulting speckle pattern shows a reduction in the Fourier power for short wavelengths in all directions, but not for the longer wavelengths that are determined by the speckle size

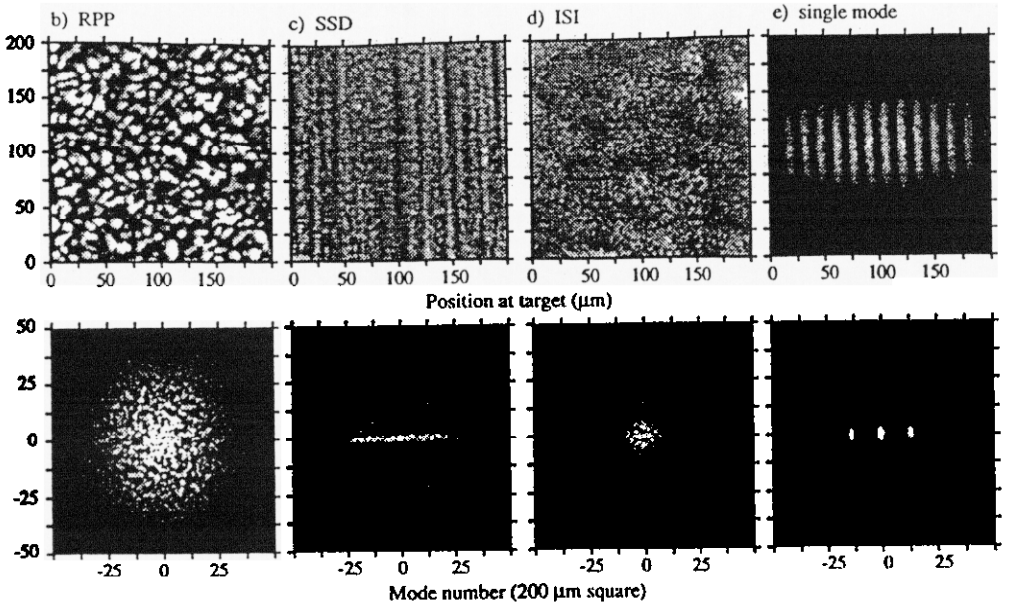

Figure 1: Optical irradiation patterns used for the imprint experiments. The patterns shown are a) static RPP speckle pattern, b) SSD smoothed speckle pattern, c) ISI smoothed speckle pattern, and d) 15 μm single optical mode. Each is displayed as modulation in exposure on the film. The 2-D Fourier transforms are shown for reference.

for the beamlets from each segment of the glass plate array. We measured an rms modulation of 0.27 for the ISI smoothed speckle pattern.

The differences in the speckle patterns are illustrated with lineouts in Fig. 2 of the 2-D Fourier spectra shown earlier in Fig. 1. Lineouts of Fourier power parallel and perpendicular to the dispersion direction show that the power in the perpendicular direction is only slightly reduced from the static speckle pattern, whereas the power in the parallel direction is significantly reduced by the time-varying dispersion. For the case of ISI smoothing, the power is reduced for wavelengths shorter than about 50 μm (mode 4) in all directions.

LASER IMPRINTED MODULATION

A. 0.53 μm irradiation at 2-6x10^{12} W/cm^2

We irradiated 2 μm thick Al foils with a 1 ns laser pulse at intensities varying from 2-6x10^{12} W/cm^2 at 0.53 μm. The typical shock breakout time is about 0.20 ns. We recorded XUV radiographs of the modulation in optical depth in the foil using the Ge x-ray laser. An extensive data set was obtained including both imprint and subsequent R-T growth by recording radiographs at various times relative to the imprint laser pulse.

We show sample XUV radiographs in Fig. 3 that were recorded for each smoothing scheme on Vulcan. These are all shown at about 0.45 ns into the optical drive pulse, following 0.25 ns of R-T instability growth. In the case of static speckle, the modulation in optical depth of the foil is very pronounced. For the SSD and ISI smoothed cases with measured optical exposure rms modulations of 0.25-0.27, however, the modulation is close to the level of the background resulting from the surface finish of the Al foils and the intrinsic speckle pattern of the x-ray laser at the plane of the thin foil.

Two-dimensional Fourier transforms of the optical depth modulation are also shown in Fig. 3, corresponding to the XUV radiographs. These show structure that reproduces the structure of the optical speckle patterns, shown earlier in Fig. 1. Lineouts of these 2-D Fourier power are shown in Fig. 4. Two lineouts are shown for the SSD smoothed beam parallel and perpendicular to the dispersion direction, whereas the lineouts for the static and ISI smoothed imprint are azimuthally symmetric and are shown averaged for the two directions. The modulation imprinted by an SSD smoothed beam shows power at short wavelengths only in the direction perpendicular to the dispersion direction. For the example of ISI, the lineout shows power at long wavelengths characteristic of the speckle from the individual echelon segments, but there is little power in short wavelength modulations in all directions, as shown previously for the lineouts of the Fourier transform of the optical speckle pattern.

By imaging the optical depth modulation of the thin Al foil at a range of times, we record the R-T growth of perturbations in the foil. We show a time sequence of lineouts from the Fourier analysis of the static speckle imprinted modulations in Fig. 5. This shows the growth of perturbations at all wavelengths. Note that because the Fourier transforms are azimuthally symmetric, we can multiply these curves by $2\pi n$, where n is the mode number, to obtain Fourier power per mode. This then provides a technique for measuring of the instability growth, resolved as function of mode number.

Since we do not yet have detailed simulations of this experiment that include opacity effects ($\kappa=\kappa(\rho)$), we

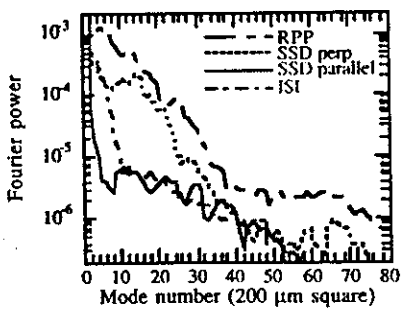

Figure 2: Linouts of the 2-D Fourier transforms showing the reduction in power per mode due to SSD and ISI smoothing of the laser speckle pattern.

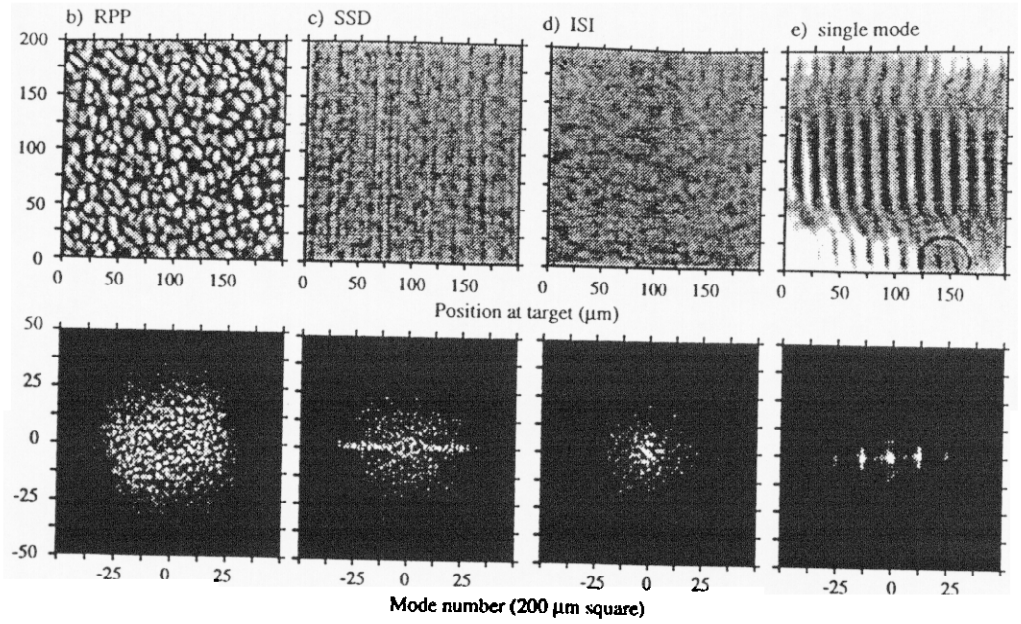

Figure 3: XUV radiographs of modulation in the Al foil recorded with the x-ray laser. These are shown as modulation in optical depth at t=0.45 ns for the cases a) static speckle imprint, b) SSD smoothed imprint, and c) ISI smoothed imprint. The modulation in optical depth imprinted by a single 15 μm mode is shown at t=0.58 ns. Two-dimensional Fourier transforms are shown for reference.

empirically normalized our measurements to correct for the average change in opacity due to compression (discussed in the following section). This normalized rms is plotted in Fig. 6 for the various cases of laser smoothing. Details of the change in rms as a function of time depends on the Fourier composition of the speckle pattern. However, as a first order approximation, we assume the growth rate is the same for the different cases, and an exponential fit to the static imprint data is applied with a constant multiplier to the other two cases. We observe significant imprint of the static speckle. Interpolating at the shock breakout time of about 0.20 ns, we observe that the fractional rms modulation in mass per unit area is 0.053±0.009.

The SSD smoothed case shows little change in the rms above the noise early in time. We can see the 1-D modulation characteristic of the residual speckle pattern due to SSD smoothing, but the isotropic noise due to the surface finish of the foil and the intrinsic speckle pattern of the x-ray laser dominates the rms. The surface roughness of the Al foils is about 20 nm, which corresponds to a level of 0.01 in Fig. 6.

At late time, the modulation imprinted by SSD grows above the noise level. If we look at t=1.0 ns, and extrapolate back to shock breakout at 0.20 ns by assuming the same R-T growth history as for the static RPP speckle case (curve shown in Fig. 6), then we obtain an rms modulation in fractional mass per unit area of 0.018±0.002. The growth rate does depend weakly on the distribution of modes, but we have not included this in our initial analysis of the data.

Performing a similar analysis on the data obtained by imprinting with ISI, we observe that the rms modulation in fractional mass per unit area is about 0.008±0.001 at t=0.20 ns. The ISI smoothed speckle pattern imprints the least in these targets. Note that in this case the pulse shape has a rise time that is >0.2 ns due to the glass plate beam delays. The different pulse shape may affect the overall hydrodynamics, but relative to the 50% rise point on the laser pulse shape, the shock breaks out at the same time (0.2 ns).

B. Single mode 0.53 μm irradiation

By introducing a beam block with two small apertures, as described separately,[9] we imprinted a hydrodynamic perturbation into the foil with a single wavelength. We used this to characterize single mode imprinting and R-T growth, and also to characterize the opacity increase for shock compressed Al. Although we conducted a sequence of tests, using single mode optical perturbations with wavelength of 15-90 μm, and at 1-10x10^{12} W/cm^2, we discuss here only a summary of the results from the 15 μm single optical mode imprinting at 3-5x10^{12} W/cm^2, and we compare the results with the multiple mode imprinting. Detailed analysis of the different cases is shown in more detail by Wolfrum et al.[9]

An XUV radiograph of a thin Al foil imprinted with this λ=15

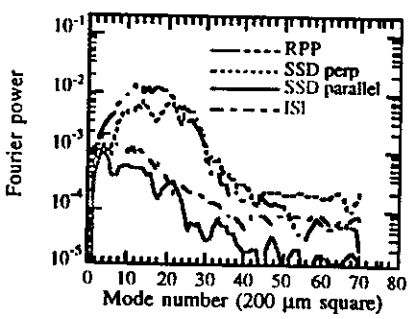

Figure 4: Lineouts of Fourier power from XUV radiograh of multiple mode laser imprint shown earlier in Fig. 3.

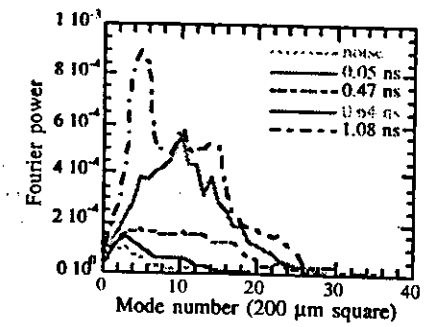

Figure 5: Fourier power per mode plotted at a range of times, showing the growth per mode.

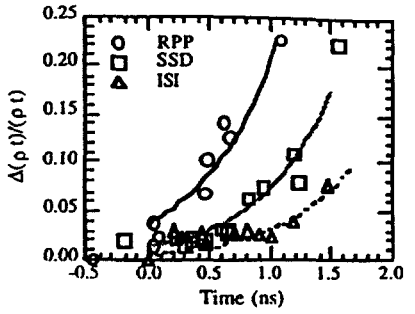

Figure 6: Modulation in optical depth as a function of time imprinted by the different smoothing techniques.

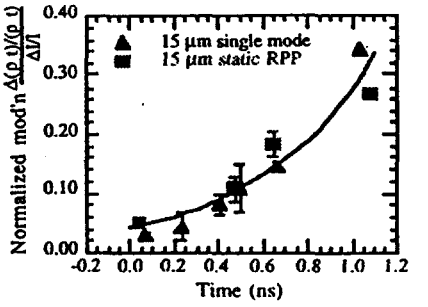

Figure 7: Imprint efficiency measured from both single mode and multiple mode optical modulations for λ=15 μm.

μm single mode pattern at about 3×10^{12} W/cm^2 is shown in Fig. 3d, along with the two dimensional Fourier transform. The zero order interference fringe intensity pattern has an Airy pattern envelope with fwhm dimension of the central peak of about 125 μm x 320 μm. This image, recorded at 0.58 ns into the optical drive pulse, shows a single mode modulation in the optical depth of the foil.

The x-ray laser probe allows us to radiograph a large area of the foil that includes both shocked and unshocked regions when we use a small irradiation pattern such as that generated with the two apertures. We observe in the radiographs that the shocked region is more opaque than the unshocked region (the region with the ripples in Fig. 3d is darker on average than the surrounding edges), which is due to a shock enhancement in the opacity.

We quantify the shock change in opacity using a time-sequence of radiographs, and empirically remove the effect of time-dependent opacity from the rms modulation of the imprinted foil, as shown earlier in Fig. 6. We apply this correction as:

$$\frac{\delta(\rho t)}{(\rho t)} = \frac{\delta(\ln(exposure))}{(\kappa\rho t)_o + \Delta(OD)},$$

where $(\kappa\rho t)_o$ is 4.48 for 2 μm thick cold Al at the 19.6 nm Ge x-ray laser wavelength, and $\Delta(OD)$ is the difference in average optical depth in the shocked region vs. the unshocked region. In these experiments, the average change in optical depth, $\Delta(OD)$, is <1.3 in the shocked region, which means that this effect represents a correction to the fractional modulation of mass per unit area less than 25%.

Note that once the shock breaks out from the Al foil at 0.20 ns, the effect of shock enhancement of the opacity is reduced because the foil decompresses. Calculations with OPAL result in a change in the opacity of the Al of 25% during the shock transit phase, in agreement with the experimental result. After shock breakout, however, simulations that included x-ray preheat suggested the foil decompressed faster than the opacity data indicates. At the time of shock breakout, the simulations indicated that the ratio of P/P(Fermi) at the high pressure limit was about 1.03. Several hundered ps after the shock breaks out, x-ray preheat has a larger effect, but this does not affect the comparison of imprinted modulation due to the different smoothing schemes since they are affected identically. This effect of preheat is a complication of the experiments, but it does not invalidate them as a test of the modeling.

We Fourier analyzed the modulation imprinted by the single mode optical pattern for the experiments, and plotted the Fourier amplitude of the 15 μm mode as a function of time. This is shown in Fig. 7, corrected for the change in opacity due to shock compression, and normalized by the laser intensity modulation of the 15 μm mode obtained by Fourier analyzing the optical intensity pattern shown earlier in Fig. 1d. This corresponds to an imprint efficiency.

The single mode and multimode perturbations are imprinted in the foil with similar efficiency relative to the optical intensity modulation, demonstrating the linearity of the imprint process in these experiments. On the graph, we include a fit to the full set of data, including the single mode and multiple mode results at average intensities of $3\text{-}5\times10^{12}$ W/cm^2. The growth rate plotted here is 1.9±0.2 ns^{-1}, where the growth is of modulation normalized to the laser intensity modulation.

SUMMARY AND CONCLUSIONS

We have used the XUV radiography technique to study imprint in thin foils. We made measurements of the temporal development of the imprinted modulation including Rayleigh-Taylor growth of the modulations imprinted by low intensity 0.53 μm irradiation on a 2 μm Al foil under various laser smoothing schemes. We have used a single mode intensity pattern to characterize the imprint at single perturbation wavelengths. This allows a direct comparison of single vs. multiple mode imprinting.

ACKNOWLEDGMENTS

We gratefully acknowledge the support from the Vulcan laser support staff throughout these experiments. This work was funded by the Engineering and Physical Sciences Research Council. It was also partially supported under the auspices of the US DOE by LLNL under Contract No. W-7405-ENG-48, and EW was supported by the Austrian Fonds zur Förderung der wissenschaftlichen Forschung under Project No. P10844 NAW.

REFERENCES

[1]J. M. Soures, J. Fusion Energy **10**, 295 (1991).

[2]S. W. Haan *et al*, Phys. Plasmas **2**, 2480 (1994).

[3]Y. Kato *et al*, Phys. Rev. Letters **53**, 1057 (1984).

[4]S. Skupsky *et al*, J. Appl. Phys. **66**, 2456 (1989).

[5]R. H. Lehmberg *et al*, Opt. Commun. **46**, 27 (1983); D. A. Peplar *et al*, Proc. SPIE **1840**, 76 (1993).

[6]H. Nakano *et al*, J. Appl. Phys. **73**, 2122 (1993); N. Miniyaga *et al*, to appear in Proc. 15th IAEA Conf., Vienna.

[7]D. H. Kalantar *et al*, Rev. Sci. Instrum. **68**, 802 (1997); D. H. Kalantar *et al*, Phys. Plasmas **4**, 1985 (1997).

[8]D. G. Stearns *et al*, J. Vac. Sci. Technol. A **9**, 2662 (1991); T. W. Barbee, Jr. *et al*, Appl. Opt. **32**, 4825 (1993).

[9]E. Wolfrum *et al*, submitted to Phys. Plasmas; E. Wolfrum *et al*, these proceedings.

Technical Information Department • **Lawrence Livermore National Laboratory**
University of California • Livermore, California 94551